IL NUOVO CIMENTO **44 C** (2021) 64
DOI 10.1393/ncc/i2021-21064-y

COMMUNICATIONS: SIF Congress 2020

High-resolution X-ray imaging as a powerful diagnostics tool to investigate in-plasma nuclear β-decays

E. NASELLI(1)(2) S. BIRI(3) L. CELONA(1) A. GALATÀ(4) S. GAMMINO(1) M. MAZZAGLIA(1) R. RACZ(3) G. TORRISI(1) and D. MASCALI(1)

(1) *INFN, Laboratori Nazionali del Sud - Catania, Italy*
(2) *Dipartimento di Fisica e Astronomia, Università degli Studi di Catania - Catania, Italy*
(3) *Institute for Nuclear Research (ATOMKI) - Debrecen, Hungary*
(4) *INFN, Laboratori Nazionali di Legnaro - Legnaro, Italy*

received 15 January 2021

Summary. — In the frame of the PANDORA_Gr3 (Plasmas for Astrophysics, Nuclear Decay Observation and Radiation for Archaeometry) project aiming at measuring in-plasma nuclear β-decays of astrophysical interest, a multi-diagnostic approach to correlate plasma parameters to nuclear activity has been performed. High-resolution spatially resolved X-ray spectroscopy, by means of an X-ray pin-hole camera setup, represents a powerful method for plasma structure evaluation. Innovative algorithms for analyzing photon-counting images to perform energy-resolved investigation pixel by pixel have been developed and deep investigations about confinement dynamics are also possible, distinguishing fluorescence lines of each material of the plasma chamber (titanium, tantalum) from fluorescence lines of plasma (argon).

1. – Introduction

Magnetized ECR (Electron Cyclotron Resonance) plasmas in compact traps may become experimental environments for the investigation of nuclear β-decays of isotopes of nuclear astrophysical interest. Theoretical predictions and former experiments showed that the ionization state can modify, even by several orders of magnitude, the isotopes lifetimes τ [1-4]. The PANDORA_Gr3 project [5, 6] proposes a new approach aiming at measuring, for the first time, the influence of the plasma charge state distribution (CSD) and the other parameters (*i.e.*, plasma density n_e and temperature T_e) on the nuclear decay τ [7]. In the PANDORA_Gr3 plasma trap the radionuclides can be trapped in a dynamic equilibrium, living for days or even weeks with on-average constant local n_e and T_e ($n_e \sim 10^{11} - 10^{13}\,\mathrm{cm}^{-3}$, $T_e \sim 0.1 - 100\,\mathrm{keV}$). An innovative multi-diagnostic setup [8, 9] has been developed and allows to reach unprecedented plasma proprieties investigation.

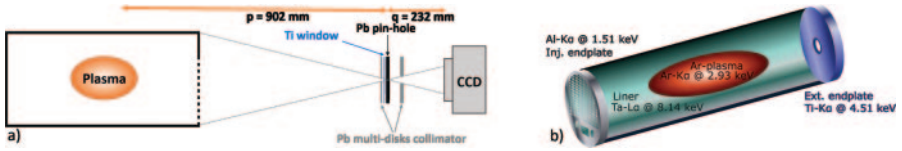

Fig. 1. – Sketch of the X-ray pin-hole camera setup (a) and of the plasma chamber (b).

Among the others, the powerful X-ray pin-hole camera system is able to perform high-resolution space-resolved spectroscopy and spectrally resolved imaging, allowing confinement dynamics studies and plasma morphology and structure investigations.

2. – Experimental setup

The design of the PANDORA_Gr3 plasma trap is ongoing and the measurements here presented were carried out in the 2nd-generation ECRIS installed at ATOMKI, in Debrecen [10]. The non-invasive diagnostic system, shown in fig. 1(a), consists of:

- a *CCD camera* (sensitive range 2–20 keV, 1024 × 1024 pixels, sensor size 13.3 × 13.3 mm);
- a *Pb pin-hole* of 2mm of thickness (t) and 400 μm of hole diameter ($\emptyset_h$), able to reproduce the plasma image in the CCD; the magnification was optimized at 0.24;
- a *Ti window* ($t = 9.5\,\mu$m) to reduce UV and visible light and a *multi-disks collimator* consisting of two Pb disks ($t = 1\,\text{mm}, \emptyset_h$: 1 and 2 mm). It has been specially designed to remarkably increase signal-to-noise ratio at relatively high RF-power mode, up to 200 W [11] (previous measurements were performed only up to 30 W [12, 13]).

A special design of the plasma chamber walls covered by a liner of Ta (lateral walls) and Ti and Al (extraction and injection endplate, respectively) has been implemented to distinguish fluxes of X-rays coming from walls' bremsstrahlung and fluorescence (produced by the electrons escaping the trap and impinging on the metals surfaces) from the ones coming from the Ar plasma (due to the fluorescence of confined ions). The plasma chamber is sketched in fig. 1(b), the perspective front view in fig. 2(a). The mesh structure of the Al plate ($\emptyset_{wire} \sim 400\,\mu$m) guarantees 60% of optical X-ray transmission.

3. – Experimental results

The photon impinging in the CCD generates a charge proportional to the deposed energy. The Analogue Digital Unit (ADU) is proportional with the product of the incident photons and their energies. Typically, there are two main operative modes to acquire the images: the *Spectrally Integrated (SpI) mode* and the *Photon Counting (PhC) mode*.

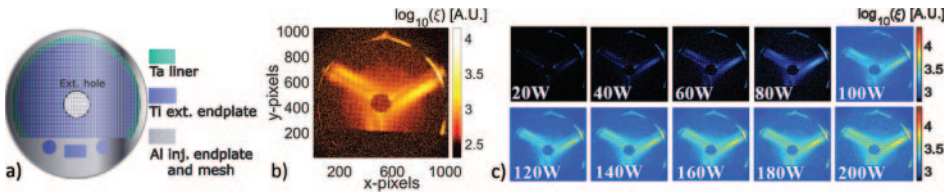

Fig. 2. – (a) Perspective front view of the plasma chamber. (b) Typical SpI X-ray image. (c) Pseudo-color SpI images (same logarithmic scale): power scaling from 20 W to 200 W, step 20 W.

3˙1. *SpI X-ray imaging.* – During a long t_{exp} (exposure time) —images collected for several tens of seconds— multi-events are registered by the CCD camera, and the spectral information of the incoming X-rays is lost. Therefore, images obtained with long t_{exp} are called SpI images. In this case energy separation of the events is not possible, however, the ADUs reveal the energy content (ξ) of the plasma and the energy released as bremsstrahlung radiation caused by fluxes of deconfined electrons impinging on the plasma chamber walls, also including the fluorescence of the chamber materials.

These acquisitions are typically fast (tens of seconds) and it is thus possible to infer, likely *on line*, the changes of plasma morphology. In fig. 2(b) a typical SpI X-ray plasma image is shown ($t_{exp} = 50\,\mathrm{s}$, at 1 MHz of readout rate). It is possible to recognize the lateral wall of the plasma chamber, the extraction hole and both the shadows caused by the mesh structure and the bulk Al of the injection plate. An example of the power dependence of the SpI images is shown in fig. 2(c), for a pumping RF power from 20 W to 200 W: changes to the ξ of the plasma are clearly visible. By selecting specific ROIs in the images it is possible to quantitative investigate about the ξ of the emission.

3˙2. *PhC imaging and space-resolved spectroscopy.* – The more powerful investigations, able to perform local energy determination, is provided by single PhC mode. Decoupling of photon number *vs.* energy is, this way, possible. The technique allows to perform space-resolved spectroscopy, thus evidencing the local displacement of electrons at different energies, as well as of plasma ions highlighted by fluorescence lines emission. The PhC mode is obtained by fixing a short t_{exp} for each of the acquired image frame (in the range of tens of ms). Multi-images are recorded in PhC (of the order of thousands image frames). The PhC mode allows minimizing the probability that two (or more) photons hit the same pixel during the t_{exp} of a single image frame with consequent loss of information about their energies. Only a few number of pixels are illuminated on the full CCD matrix and they can be associated with single photon events and, consequently, they carry the information (in terms of charge) on the energies of the incident photons. To elaborate PhC images, advanced analytical methods have been developed.

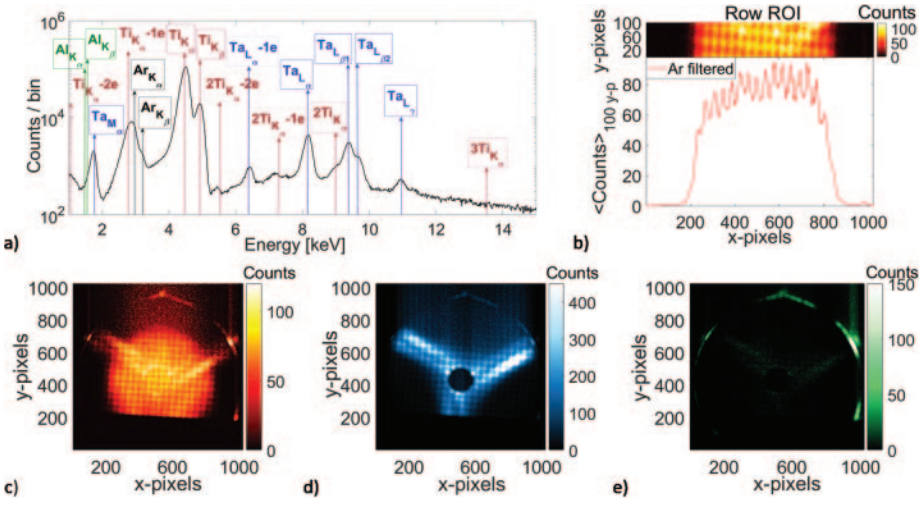

Fig. 3. – (a) Full-field X-ray spectrum. (b) Intensity profile evaluated along a ROI of [100 × 1024] pixels of the Ar-filtered image. Energy-filtered images showing fluorescence photons coming from Ar plasma (c) and from the metallic layers covering plasma chamber: Ti (d) and Ta (e).

Figure 3(a) reports a typical full-field X-ray spectrum. The thousands of image frames gain the statistics necessary for elaborating high-quality X-ray fluorescence spectra and images. It is possible to distinguish fluorescence lines of each material of the plasma chamber (Ti, Ta) and the fluorescence lines of plasma (Ar). There are also dimer and escape peaks for each fluorescence line. The energy resolution is 0.326 keV at 8.1 keV [9]. Characteristic peaks in the X-ray spectra, coming from each material, allow to study the confinement dynamics (plasma *vs.* losses X-ray emission) discriminating the radial losses from the axial losses. X-rays coming from magnetic branches (where electrons are axially deconfined) consist of mostly fluorescence from Ti, X-rays coming from plasma are mostly due to ionized K_α Ar lines and X-rays coming from poles (where electrons are radially deconfined) are mostly due to radial losses impinging on the Ta liner. Since the data on the spectrum contains the spatial information on the emitting positions, the definition of a ROI on the fluorescence peaks in the spectrum allows the imaging of the elemental distribution. As highlighted in fig. 3(c)–(e), it is possible to distinguish the emission coming from Ar plasma only (selecting the fluorescence from Ar, fig. 3(c)), compared to the axial losses (Ti, fig. 3(d)) or the radial losses (Ta, fig. 3(e)), selecting the fluorescence from Ti and Ta, respectively. Moreover, the intensity profile along a ROI of $[100 \times 1024]$ pixels has been evaluated in the Ar-filtered image (fig. 3(b)). It is possible to well distinguish the Al mesh structure, highlighting the high spatial resolution ($500\,\mu$m).

Also the plasma radius was evaluated: $r_p = 15.53 \pm 0.87$ mm, compatible with the radius expected (15.50 mm) considering the realistic magnetic field profile confining the plasma.

4. – Conclusion and perspectives

The paper reports the tool, the method and the experimental results of a powerful system for making plasma physics investigation by means of space-resolved spectroscopy. Integrated imaging allows live plasma structure and emission investigations. The more powerful analysis consists in the spatial-resolved spectroscopy for quantitative estimation of deconfined fluxes, locally elemental composition and plasma parameters (n_e, T_e) measurements. It will be very useful for the PANDORA_Gr3 project, for plasma volume V_p on-line evaluation (τ directly depends on V_p) and for plasma parameters monitoring.

* * *

The authors gratefully acknowledge the support of INFN by the Grants PANDORA (5th Nat. Comm.) and PANDORA_GR3 (3rd Nat. Comm.).

REFERENCES

[1] Litvinov Y. and Bosch F., *Rep. Prog. Phys.*, **74** (2011) 016301.
[2] Takahashi *et al.*, *Phys. Rev. C*, **36** (1959) 1522.
[3] Bosch F. *et al.*, *Phys. Rev. Lett.*, **77** (1996) 5190.
[4] Jung M. *et al.*, *Phys. Rev. Lett.*, **69** (1992) 2164.
[5] Mascali D. *et al.*, *EPJ Web of Conferences*, **227** (2020) 01013.
[6] Mascali D. *et al.*, *Eur. Phys. J. A*, **53** (2017) 145.
[7] Naselli E. *et al.*, *EPJ Web of Conferences*, **227** (2020) 02006.
[8] Biri S. *et al.*, *J. Instrum.*, **13** (2018) C11016.
[9] Naselli E. *et al.*, *J. Instrum.*, **14** (2019) C10008.
[10] Biri S. *et al.*, *Rev. Sci. Instrum.*, **83** (2012) 02A341.
[11] Biri S. *et al.*, *J. Instrum.*, **16** (2021) P03003.
[12] Rácz R. *et al.*, *Plasma Sources Sci. Technol.*, **26** (2017) 075011.
[13] Mascali D. *et al.*, *Rev. Sci. Instrum.*, **87** (2016) 02A510.